Book Chapter

Evolution of Strength Parameters for Sandstone Specimens during Triaxial Compression Tests

Xiang Ding[1,2,3]*, Na Chen[1], Fan Zhang[1,2,4] and Guangqing Zhang[4]

[1]School of Civil Engineering Architecture and Environment, Hubei University of Technology, Wuhan, China
[2]Sino-French Joint Research Center of Rock, Soil Mechanics & Concrete Materials, Hubei University of Technology, Wuhan, China
[3]Laboratory of Multiscale and Multiphysics Mechanics-LaMcube-CNRS FRE 2016, Lille F59655, France
[4]Department of Engineering Mechanics, China University of Petroleum-Beijing, Beijing, China

***Corresponding Author:** Xiang Ding, School of Civil Engineering Architecture and Environment, Hubei University of Technology, Wuhan, China

Published **May 09, 2024**

This Book Chapter is a republication of an article published by Xiang Ding, et al. at Advances in Civil Engineering in June 2021. (Xiang Ding, Na Chen, Fan Zhang, Guangqing Zhang. Evolution of Strength Parameters for Sandstone Specimens during Triaxial Compression Tests. Advances in Civil Engineering. Volume 2021, Article ID 8856743, 11 pages. https://doi.org/10.1155/2021/8856743)

How to cite this book chapter: Xiang Ding, Na Chen, Fan Zhang, Guangqing Zhang. Evolution of Strength Parameters for Sandstone Specimens during Triaxial Compression Tests. In: Mohamed Ali Hajjaji, editor. Prime Archives in Engineering. Hyderabad, India: Vide Leaf. 2024.

Abstract

Despite the lack of test data of the coefficient of pressure sensitivity α and the shearing cohesion k, the Drucker–Prager criterion is commonly applied for numerical analyses of geotechnical engineering. To bridge the gap between the wide application and insufficient knowledge of strength parameters of the Drucker–Prager criterion, this study presents experimentally calibrated strength parameters of this criterion for the first time. This paper proposes a new method to measure α and k in the Drucker–Prager criterion. The square root of the second invariant of the deviatoric stress tensor $\sqrt{J_2}$ is linearly fitted with the first invariant of the stress tensor I_1 in the stress space. The parameters φ and c in the Mohr–Coulomb criterion and α and k in the Drucker–Prager criterion are calibrated to the same set of triaxial compression tests of sandstones. With these testing results, five pairs of conversion formulae (which are most commonly used in the literature) are examined and the most appropriate pair of conversion formulae is identified. With parameters indicating cohesive strength (c and k) and parameters indicating frictional strength (φ and α), the evolutions of different strength components are compared with those in the cohesion-weakening friction-strengthening model. With an increase in plastic deformation, the cohesive strength parameters c and k firstly increase to a peak value and then decrease. The frictional strength parameters φ and α gradually increase at a decreasing rate after the initial yield point.

1. Introduction

The Mohr–Coulomb criterion and the Drucker–Prager criterion are often used in geotechnical engineering. The Mohr–Coulomb criterion assumes that the shearing stress on the failure plane is a function of the normal stress on the failure plane, which is expressed as [1–3]

$$\tau = \tan \varphi \cdot \sigma + c, \tag{1}$$

where τ represents the shearing stress on the cross section, σ represents the normal stress on the cross section, φ represents the angle of internal frictional, and c represents the cohesion. However, the Mohr–Coulomb failure criterion has three main shortcomings. First, it assumes that the intermediate principal stress does not influence failure1, 4–8; second, the meridians and the failure envelope in Mohr's diagram are straight lines, which implies that the strength parameter φ does not change with the confining pressure [9, 10]; and third, the failure surface in the stress space has corners, which are difficult to handle in a numerical analysis [11].

Drucker and Prager [12] considered the Mises criterion and modified it to the Drucker–Prager criterion, as expressed in the following equation:

$$\sqrt{J_2} - \alpha I_1 - k = 0, \tag{2}$$

where J_2 represents the second invariant of the deviatoric stress tensor, α represents the coefficient of pressure sensitivity, I_1

represents the first invariant of stress tensor, and k represents the shearing cohesion (for the parameters α and k that have not been named in the list of symbols suggested by ISRM [13], this paper used k as the shearing cohesion in order to distinguish it from the cohesion c in the Mohr–Coulomb criterion, and α as the coefficient of pressure sensitivity).

The Drucker–Prager criterion, which is continuously differentiable (except for the cone top in the stress space), is commonly preferred by many numerical analysis software sets, despite the various limitations associated with the Drucker–Prager criterion [14–16]. However, when the Drucker–Prager criterion is used for numerical analysis, no test parameters are available for the coefficient of pressure sensitivity α and the shearing cohesion k. Therefore, these have to be indirectly obtained from the angle of internal friction φ and cohesion c (which can usually be identified by conducting triaxial compression tests) by conversion through conversion formulae [14, 16, 17]. The parameters c and φ of the Mohr–Coulomb criterion have been intensively studied and numerous models have been proposed to describe the evolution of c and φ during the plastic deformation stage [18–32]. Both parameters are of vital importance in geotechnical engineering stability analyses, especially for tunnel design [33–38]. However, little test data is available for the parameters α and k except for the result reported by Yao [39], who measured those parameters semiempirically by a rather complicated deduction of formulae and processing of experimental data. It should be noted that Yao observed an increase of k at the later stage of plastic deformation, which implies that the internal cohesive strength increases with increasing plastic deformation. Yao's conclusion may, however, be doubted, as it implies that the bonding of particles will be strengthened even if a macro failure plane has emerged. According to the different spatial relationships of the Mohr–Coulomb criterion and the Drucker–Prager criterion in the stress space, several kinds of conversion formulae can be applied for the parameters of these two criteria, and these different conversion formulae also yield different results [40–44]. According to Zheng et al. [44], with different formulae to calculate the parameters α and k, the deviation in the ultimate bearing capacity of geomaterials may deviate as much as 500%. Xiong and Zhang [45] studied the influence of different conversion formulae on the conversion of φ and c to α and k (in an analysis of the safety of dams). The authors suggested that, in numerical analysis, different conversion formulae should indeed be adopted according to different strength safety factor needs.

The conversion formulae for the parameters in the Mohr–Coulomb and Drucker–Prager yield criteria were explained from the principle of minimal deviation of energy [42]. Because of the deviations that would emerge if the Mohr–Coulomb hexagon were to be approximated as either inscribed or circumscribed by the Drucker–Prager circle, a new pair of conversion formulae was proposed [46]. This pair was proposed by assuming that the Drucker–Prager circle would have the same area as of the Mohr–Coulomb hexagon on the π plane. The proposed conversion formulae were validated by engineering practices. By numerical simulation, Deng et al. [47] concluded that the different conversion formulae between the Mohr–Coulomb criteria and the Drucker–Prager criterion would significantly influence the simulation results. Using a finite element model in ANSYS, Chen et al. [48] computed the displacements and stresses of a slope after excavation under two conditions; i. e., the Mohr–Coulomb vertices were either inscribed or circumscribed by the Drucker–Prager circle. The results under the condition of the inscribed Drucker–Prager circle were much closer to the results obtained by the Mohr–Coulomb criterion. As an alternative way of getting the parameters α and k, Zhang proposed that the parameters α and k can be measured by true triaxial tests under different stresses and strain states. Zhang further suggested that the fitting of α and k should be in accordance with the stress state existing in practical engineering. If different values of α and k were adopted, the limiting load might deviate by as much as 400%, so the values of α and k should be selected with care.

Although the Drucker–Prager criterion is often utilized in various applications of geotechnical engineering, its parameters are usually converted from the Mohr–Coulomb criterion and the calibrated parameters of the Drucker–Prager are rarely reported. Moreover, the evolution of the strength parameters is highly important for the analysis of the progressive failure of underground caverns [18, 19]; however, the evolution of the strength parameters of Drucker–Prager criterion during the plastic deformation process has not been calibrated to date. Hence, in this paper, for the same group of triaxial compression tests in different stress spaces, the parameters α and k are calibrated in the Drucker–Prager criterion and the parameters φ and c are calibrated in the Mohr–Coulomb criterion for the same group of triaxial compression tests in different stress spaces. The evolutions of parameters α , k, φ, and c are studied with plastic deformation. Moreover, the disparities of different conversion formulae of the Drucker–Prager criterion and the Mohr–Coulomb criterion are examined with the calibrated strength parameters.

2. Complete Stress-Strain Curve and Strength Curve

2.1. Complete Stress-Strain Curve of Tight Sandstone under Triaxial Compression. To obtain the parameters c and φ in the Mohr–Coulomb criterion and α and k in the Drucker–Prager criterion, triaxial experiments were conducted in the laboratory of rock mechanics at the China University of Petroleum-Beijing (CUPB).

Three cylindrical rock specimens with dimensions of ϕ25×50 mm were subjected to different confining pressures of 10 MPa, 15 MPa, and 30 MPa for triaxial compression tests. The displacement control mode was adopted to acquire the complete stress-strain curve including both the hardening stage and the softening stage. A fluid-servo rock testing system, TFD-1000, available at the CUPB, was utilized, which is fully able to conduct the triaxial compression tests. The electro-hydraulic servo rock testing machine had a stiffness exceeding 10 GN/m.

The three samples ($\phi 25 \times 50$ mm) were drilled from a ϕ 100 mm core taken from a tight oil reservoir of the Changqing Oil field located in the northwest of China. There were no visible cracks in these four samples after drilling. The maximum diameter of particles in these sand samples was far less than $1/20^{th}$ of the diameter of smaller samples (25 mm). The ends of the samples were ground, and the flatness and perpendicularity were assessed by using a vertical ruler and a right-angle ruler, respectively.

The samples were wrapped with heat-shrink tubes to isolate samples from confining fluid. The tests were performed in drained conditions, at standard laboratory humidity conditions. Axial and circumferential displacements were measured by LVDTs with a resolution of 0.0001 mm.

The test followed the ASTM standard D7012 [49]. Axial and circumferential displacements were measured by LVDTs. At the beginning of each test, the axial strain control mode was used, and the specimen was loaded at an axial strain rate of 0.001 mm/mm/s until the applied load reached approximately 70% of the expected peak load. At 70% peak load, the control mode was switched to the circumferential strain control mode, and the test was continued at a strain rate of 0.0001 mm/mm/s. The stress-strain curves for the three specimens were obtained as shown in Figure 1.

2.2. Strength Curves for Tight Sandstones in Triaxial Compression Tests. The use of the word *failure* is often ambiguous in the literature and is commonly used in a somewhat general sense, not clearly distinguishing between failure and yielding. A reason for this practice is that yield can be considered as the onset of failure [50]. In the history of rock mechanics, the Mohr–Coulomb criterion was used as a failure criterion, describing the mechanical properties of materials at their peak strengths. However, with the advent of servo-controlled testing machines with large rigidity, it is reasonable to realize that rock is also an elastoplastic material, not only a brittle material, as described by the peak strength. As an elastoplastic material, rock will also undergo strengthening and weakening, and the mechanical properties will not be constants but will rather vary with plastic deformation. To record the plastic loading history, the monotonically increasing scalar κ was introduced to represent the loading history. Strength parameters, i. e., cohesion c, angle of internal friction φ, coefficient of pressure sensitivity α, and shearing cohesion k, were mobilized with the plastic internal variable κ. The scenario represents the initial yield surface in the stress space. With increasing κ, the yield surface begins to expand. Until κ has increased to a certain value, the strength of a rock specimen reaches its peak strength, as represented by the peak point in the stress-strain curve. With the further gradual increase of κ, the rock specimen begins to soften, finally reaching a residual flow stage [51].

It is common to obtain the cohesion c and angle of internal friction φ by conducting triaxial compression tests under different confining pressures and then drawing a group of Mohr circles with the peak stresses σ_1 and the confining pressures σ_3. The slope and intercept of the straight line enveloping these circles are used to calculate the angle of internal friction φ and cohesion c.

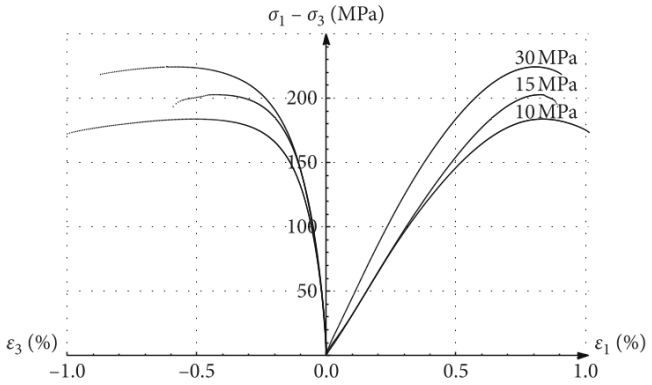

Figure 1: Stress-strain curves of triaxial compression tests under different confining pressures.

Usually, the peak strength is of major concern for designers to ensure an adequate margin of safety against failure, but there may be problems in which the postpeak behavior is also important [52]. Based on a previous analysis, the strength parameters of rocks are dependent on plastic deformation, and the constant strength parameters determined by the peak strength are only applicable to the condition of perfect plasticity. To inspect the evolution of the strength of rocks, the stress-strain curves need to be converted into curves of yield stress σ_s versus the plastic internal variable κ. These curves are usually known as strength curves.

The definition of plastic internal variable κ is not unique. For geomaterials, it can be the equivalent plastic strain, plastic work, or plastic volumetric strain [27]. Rocks are hydrostatic pressure-dependent materials and thus, plastic volumetric strains may occur during the plastic loading stage. Different from metal plasticity, which exhibits no plastic volumetric strain, the non-zero plastic volumetric strain can be regarded as a unique feature of plasticity for geomaterials. Thus, the plastic volumetric strain was selected as plastic internal variable. In this study, crack initiation was regarded as initial yield point. Various methods have been proposed to identify the onset of cracking in laboratory compression tests on rocks [53]. Here, a lateral strain response (LSR) method was utilized to determine the onset of cracking, and the details of the LSR method can be found in [54]. The initial yield points under different confining pressures were first determined by adopting the LSR method with the stress-strain curves in Figure 1. From the initial points, total strains were obtained as composed of two parts, namely, elastic strain and plastic strain. Thus,

$$\boldsymbol{\varepsilon}_{ij} = \boldsymbol{\varepsilon}_{ij}^{e} + \boldsymbol{\varepsilon}_{ij}^{p}, \tag{3}$$

where ε_{ij} represents the total strain, ε_{ij}^{e} represents the elastic strain, and ε_{ij}^{p} represents the plastic strain.

The elastic strain is calculated with Hooke's Law as

$$\boldsymbol{\varepsilon}^{e} = \mathbf{C}\boldsymbol{\sigma}, \tag{4}$$

where $\mathbf{C}$ represents the elasticity matrix and σ represents the column of principal stress vectors.

The plastic strain ε_{ij}^{p} can be obtained by subtracting the elastic strain ε_{ij}^{e} from the total strain ε_{ij} as recorded by the testing machine. Then, the plastic internal variable is expressed in terms of plastic volumetric strain by summing up the principal plastic strains [27] as

$$\kappa = \varepsilon_1^{p} + \varepsilon_2^{p} + \varepsilon_3^{p}. \tag{5}$$

By previous data processing [27], the complete stress-strain curves $\sigma - \varepsilon$ are converted into strength curves $\sigma_1^{s} - \kappa$ as shown in Figure 2. The detailed process has been explained in Wang et al. [27].

3. Fitting of the Strength Parameters of the Mohr–Coulomb Criterion and the Drucker–Prager Criterion

3.1. Fitting of the Strength Parameters of the Mohr–Coulomb Criterion. The cohesion c and the angle of internal friction φ are only constant only in perfect plasticity. However, when the Mohr–Coulomb criterion is used as a yield criterion, the cohesion c and the angle of internal friction φ are not constants anymore but vary with plastic strain. Thus, the isotropic hardening and weakening of the Mohr–Coulomb yield criterion can be expressed as

$$f\left(\sigma_1, \sigma_3, c(\kappa), \varphi(\kappa)\right) = \sigma_1 - \frac{1 + \sin\varphi(\kappa)}{1 - \sin\varphi(\kappa)}\sigma_3 - \frac{2c(\kappa)\cos\varphi(\kappa)}{1 - \sin\varphi(\kappa)}, \tag{6}$$

where σ_1 represents the maximum principal stress; σ_3 represents the minimum principal stress, i.e., the confining pressure; κ represents the plastic internal variable in terms of plastic volumetric strain in this paper; $c(\kappa)$ represents the mobilized cohesion with the plastic internal variable; and $\varphi(\kappa)$ represents the mobilized angle of internal friction with the plastic internal variable.

After the initial yield was indicated when $\kappa = \kappa_i$, there would be three yield stresses $\sigma_1^{10\text{MPa}}$, $\sigma_1^{15\text{MPa}}$, and $\sigma_1^{30\text{MPa}}$ corresponding to the confining pressures of 10 MPa, 15 MPa, and 30 MPa, respectively. According to these three pairs of $\sigma_1 - \sigma_3$ data, a straight line was fitted with the least square method as

$$\sigma_1 = K \cdot \sigma_3 + P, \tag{7}$$

where K and P are parameters of the linear fitting of $\sigma_1 - \sigma_3$.

Comparing equation (7) with equation (6),

$$K = \frac{1 + \sin\varphi(\kappa)}{1 - \sin\varphi(\kappa)}, \tag{8}$$

$$P = \frac{2c(\kappa)\cos\varphi(\kappa)}{1 - \sin\varphi(\kappa)}. \tag{9}$$

By taking $\kappa = 0.0003$ as an example, the linear fit was obtained as shown in Figure 3.

The data illustrated in Figure 3 are summarized as in Table 1.

Solving equations (8) and (9) for the data in Table 1, the cohesion and angle of internal friction were obtained as 47.1 MPa and 21.9°, respectively, when the plastic internal variable was equal to 0.0003. By repeating this process, cohesion and internal of friction at different values of plastic internal variable $\kappa = \kappa_i$ were obtained as shown in Table 2.

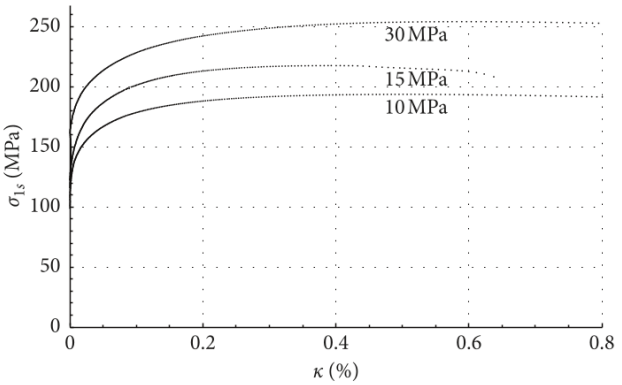

Figure 2: Yield strength vs internal plastic variable under different confining pressures.

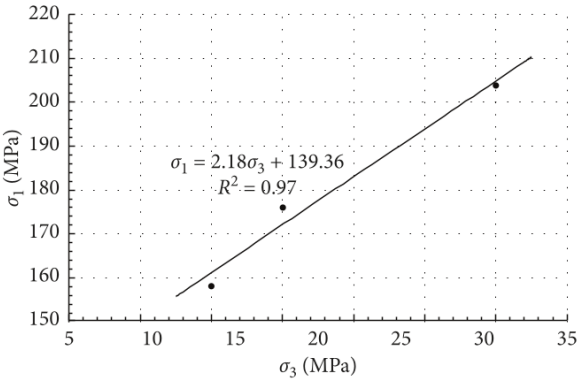

Figure 3: Linear fitting with Mohr–Coulomb criterion for $\kappa = 0.0003$.

Table 1: Linear fitting with Mohr–Coulomb criterion for $\kappa = 0.0003$.

κ ($\times 10^{-4}$)	σ_3 (MPa)	σ_{1s} (MPa)	$K(\kappa_i)$	$P(\kappa_i)$ (MPa)
	10	158.1		
3	15	176.2	2.18	139.36
	30	203.8		

3.2. Fitting of the Strength Parameters of the Drucker–Prager Criterion. Considering that the coefficient of pressure sensitivity α and the shearing cohesion k are functions of the plastic internal variable κ, the isotropic hardening and weakening of the Drucker–Prager criterion can be expressed in terms of the invariant of stress tensor, as

$$g\left(I_1, J_2, \alpha(\kappa), c(\kappa)\right) = \sqrt{J_2} - \alpha(\kappa)I_1 - k(\kappa), \tag{10}$$

where $\alpha(\kappa)$ represents the mobilized coefficient of stress sensitivity as a function of the plastic internal variable κ and

Table 2: c and φ for different plastic internal variable values.

κ ($\times 10^{-4}$)	$c(\kappa_i)$ (MPa)	$\varphi(\kappa_i)$ (°)
3	47.1	21.9
6	50.5	22.5
9	51.7	23.5
12	52.5	24.2
15	52.7	24.9
18	52.6	25.5
21	52.7	25.9
24	52.5	26.4
27	52.1	26.9
30	51.8	27.3
33	51.4	27.6
36	51.1	27.9
39	50.7	28.3
42	50.4	28.5
45	50	28.8
48	49.5	29
51	49.2	29.2
54	48.8	29.4

$c(\kappa)$ represents the mobilized shearing cohesion as a function of the plastic internal variable κ.

From equation (10), for a specific value of plastic internal variable as $\kappa = \kappa_i$, $\sqrt{J_2}$ is a linear function of I_1. Hence,

$$\sqrt{J_2} = \alpha(\kappa_i) I_1 + k(\kappa_i). \tag{11}$$

For the condition of $\kappa_i = 0.0003$, the coefficient of pressure sensitivity $\alpha(\kappa_i)$ and the shearing cohesion $k(\kappa_i)$ were obtained by fitting the linear functions between and with data for different confining pressures, as shown in Table 3.

The data in Table 3 were linearly fitted with $R^2 = 0.96$ as shown in Figure 4.

Repeating the same process, the coefficient of pressure sensitivity $\alpha(\kappa_i)$ and the shearing cohesion $k(\kappa_i)$ were obtained for different values of the plastic internal variable as shown in Table 4.

3.3. Evolution of the Strength Parameters of the Mohr–Coulomb Criterion and the Drucker–Prager Criterion. Figure 5 shows the evolution of c and φ of the Mohr–Coulomb criterion and of α and k of the Drucker–Prager criterion with the plastic volumetric strain κ. The parameter c of the Mohr–Coulomb criterion and the parameter k of the Drucker–Prager criterion represent cohesive strength, while the parameter φ of the Mohr–Coulomb criterion and parameter α of the Drucker–Prager criterion represent internal friction. The cohesion c and shearing cohesion k increased rapidly after the initial yield and reached their peak values when the plastic internal variable reached 0.0015. Thereafter, the parameters c and k decreased with increasing plastic internal variable. In contrast, the angle of internal friction φ and the coefficient of pressure sensitivity α gradually increased with increasing plastic internal variable, even though at a decreasing rate.

Table 3: Linear fitting with Drucker–Prager criterion for $\kappa = 0.0003$.

κ ($\times 10^{-4}$)	I_1 (MPa)	$\sqrt{J_2}$ (MPa)	$\alpha(\kappa_i)$	$k(\kappa_i)$ (MPa)
	178.1	85.5		
3	206.2	93.0	0.167	56.86
	263.8	100.4		

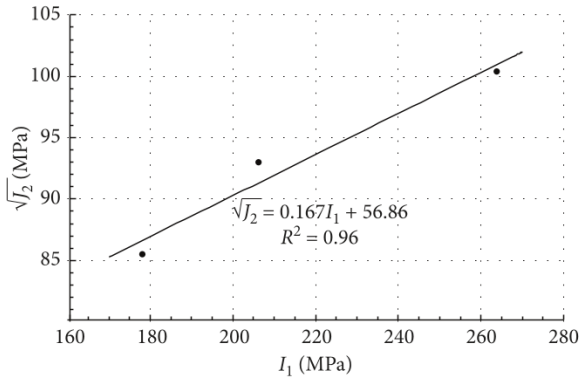

Figure 4: Linear fitting with Drucker–Prager criterion for $\kappa = 0.0003$.

Table 4: α and k for different values of the plastic internal variable.

κ ($\times 10^{-4}$)	$\alpha(\kappa_i)$	$k(\kappa_i)$ (MPa)
3	0.167	56.9
6	0.174	60.7
9	0.183	61.8
12	0.189	62.4
15	0.195	62.5
18	0.201	62.3
21	0.204	62.4
24	0.207	62.1
27	0.211	61.6
30	0.214	61.3
33	0.216	60.9
36	0.218	60.6
39	0.221	60.2
42	0.222	59.9
45	0.224	59.5
48	0.225	59
51	0.226	58.7
54	0.227	58.4

4. Conversion of Parameters of the Mohr–Coulomb Criterion and the Drucker–Prager Criterion

According to the literature, several conversion relationships exist between the parameters of the Mohr–Coulomb criterion and those of the Drucker–Prager criterion. Because of the diversity of conversion formulae, only five pairs of conversion relationships were chosen in this study as shown in Table 5. The five pairs were used to find the best fit for the tested parameters of the two yield criteria, as shown in Figure 6.

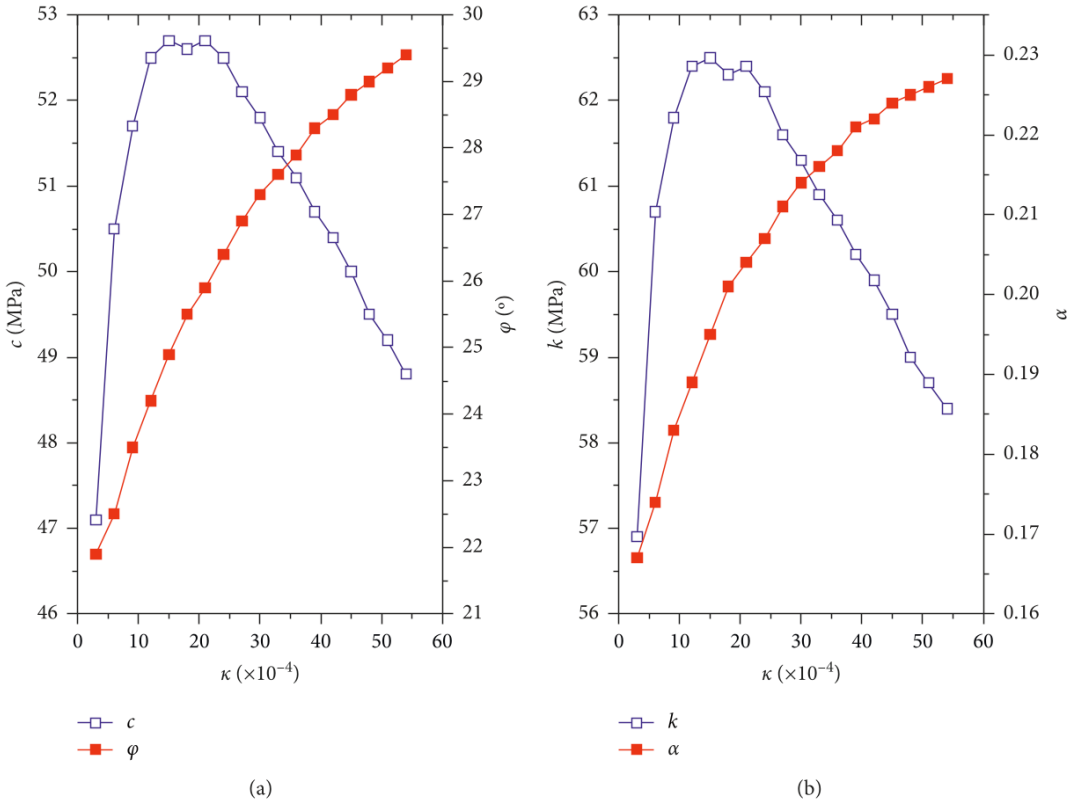

Figure 5: (a) Variation in strength parameters of the Mohr–Coulomb criterion with plastic deformation; (b) variation in strength parameters of the Drucker–Prager criterion with plastic deformation.

Table 5: Conversion relationships between the strength parameters of the Mohr–Coulomb criterion and those of the Drucker–Prager criterion.

No.	α	k	Note	Originate
1	$2\sin\varphi/\sqrt{3}(3-\sin\varphi)$	$6c\cos\varphi/\sqrt{3}(3-\sin\varphi)$	Drucker–Prager cone coincides with the outer vertices of the Mohr–Coulomb hexagon	Chen and Saleeb [41]; Chen and Liu [40]; Davis and Selvadurai [43]; McLean and Addis [55]
2	$2\sin\varphi/\sqrt{3}(3+\sin\varphi)$	$6c\cos\varphi/\sqrt{3}(3+\sin\varphi)$	Drucker–Prager cone coincides with the inner vertices of the Mohr–Coulomb hexagon	Chen and Saleeb [41]; Chen and Liu [40]; Davis and Selvadurai [43]; McLean and Addis [55]; Vee [56]
3	$\sin\varphi/\sqrt{3}\sqrt{3+\sin^2\varphi}$	$\sqrt{3}c\cos\varphi/\sqrt{3+\sin^2\varphi}$	Drucker–Prager cone inscribes with the outer vertices of the Mohr–Coulomb hexagon	Zheng et al. [44]; Chen and Liu [40]; Alejano and Bobet [14]
4	$2\sqrt{3}\sin\varphi/9-\sin^2\varphi$	$6\sqrt{3}c\cos\varphi/9-\sin^2\varphi$	Average value of case 1 and case 2	Zhang [17]
5	$2\sqrt{3}\sin\varphi/\sqrt{2\sqrt{3}\pi(9-\sin^2\varphi)}$	$6\sqrt{3}c\cos\varphi/\sqrt{2\sqrt{3}\pi(9-\sin^2\varphi)}$	On the π plane, the area of the Drucker–Prager circle equals the area of the Mohr–Coulomb hexagon.	Liu et al. [57]; Chu and Xu [42]

Figure 6 clearly shows that the first pair of conversion formulae (the Drucker–Prager cone coincides with the outer vertices of the Mohr–Coulomb hexagon) provides the best fit for the parameters of both yield parameters.

5. Discussions

5.1. Evolution Processes of Strength Components for Different Rock Types. Intuitively, a weakening of the bond of particles in rock is to be expected when the rock enters the plastic deformation stage. It should be noted that, at the early stage of plastic deformation, there is a "dramatic" increase in both the cohesion c and shearing cohesion k, as shown in Figure 5. However, many researchers have observed such an increase in the cohesion of different rock types, such as sandstone [27, 30, 31], rock salt [58], diatomaceous soft rock [22], clay [59], and granite [23]. Bishop [60] described that cohesion is contributed by two components: one is because of the inter-

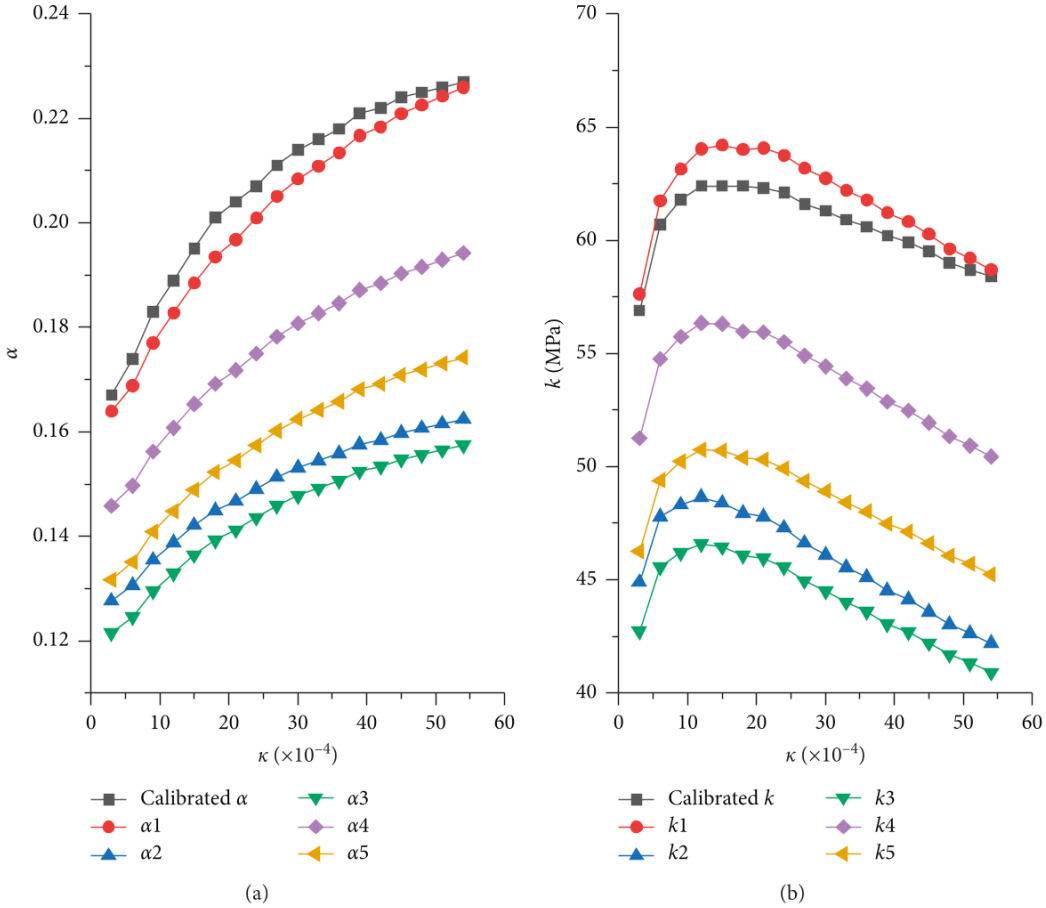

FIGURE 6: (a) Comparison of α as calculated by different conversion relationships; (b) comparison of (k) as calculated by different conversion relationships.

particle bond that developed in nature on a geological time scale and is largely destroyed by moderate shear strain or remolding; the other is a function of the void ratio present in remolded soil. This function is probably related to the physic-chemical properties of bonded water, and, as a function of strain, largely disappears on the slip surface that forms at large postpeak displacements. From this perspective, the sharp increase in cohesive strength at low strain can be considered as caused by the compactness of void in rock. Furthermore, the drop in cohesive strength emerges because an increase in plastic strain causes the bond among internal particles to continuously diminish, thus inducing the growth and accumulation of micro-cracks. From the plastic theory of rocks, the increase in cohesion can be expressed as the plastic hardening of rocks from initial yielding to peak strength.

5.2. Discussion about CWFS Model. Hajiabdolmajid proposed a cohesion weakening and friction strengthening (CWFS) model as illustrated in Figure 7 [18, 19, 61]. The model assumes that, from the onset of microcracking, the cohesive strength component of rock begins to decrease from its initial value c_i until the axial plastic strain reaches the threshold value of ε^{cp}. After that, the cohesive strength has a constant residual value c_r. The frictional strength component increases from zero at the onset of microcracking to a constant maximum friction strength at the axial plastic strain of ε^{fp}.

Since the results of the present study resemble the CWFS model, this paper briefly discusses the CWFS model in the following.

The CWFS model assumes a non-simultaneous mobilization of cohesive strength and frictional strength [18]. However, Figure 7 illustrates that the cohesive strength and the frictional strength both begin to be mobilized from the onset of microcracking. This suggests that both strengths indeed mobilize simultaneously even though in different ways. Therefore, the term "non-synchronous mobilization" may be more appropriate than "non-simultaneous mobilization."

Based on the CWFS model, Hajiabdolmajid [18] proposed a new expression of the Mohr–Coulomb yield criterion by considering the cohesion weakening and friction strengthening as

$$f(\sigma) = f(c, \bar{\varepsilon}^p) + f(\sigma_n, \bar{\varepsilon}^p)\tan\varphi. \quad (12)$$

Equation (12) suggests that the frictional strength component is a function of plastic strain as indicated by the expression, $f(\sigma_n, \bar{\varepsilon}^p)\tan\varphi$ [18]. This expression

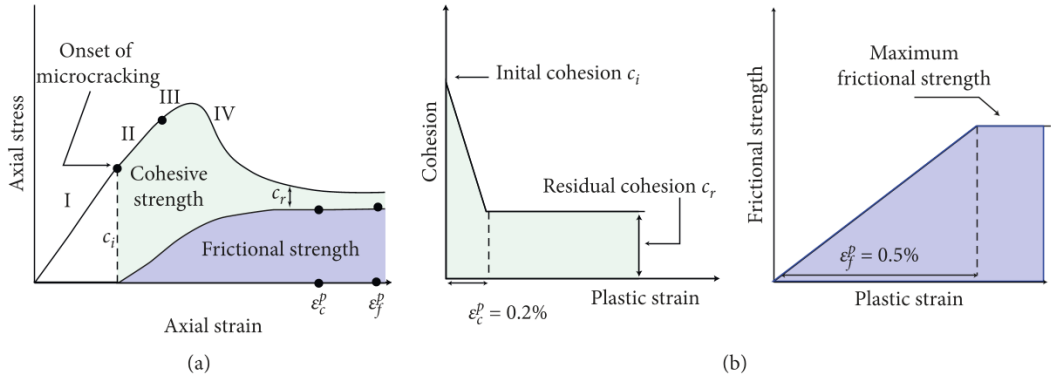

FIGURE 7: Mobilization of the strength components in the CWFS model: (a) the laboratory compression tests; (b) illustration of the cohesion loss and frictional strength mobilization as a function of plastic strain (after Hajiabdolmajid [18]).

implies that the way how normal stress is decomposed in the slip plane, rather than the angle of internal friction, is a function of plastic strain. However, in the subsequent papers by the same researcher [19, 61], the angle of internal friction was fitted as a function of plastic strain. Thus, this study proposes that equation (12) could be modified as

$$f\left(\sigma, \bar{\varepsilon}^{\mathrm{p}}\right) = c\left(\bar{\varepsilon}^{\mathrm{p}}\right) + f_1(\sigma)\tan\,\varphi\left(\bar{\varepsilon}^{\mathrm{p}}\right). \tag{13}$$

Clearly, equations (12) and (13) are different and attribute the mobilization of cohesive strength to different reasons. Since the papers by Hajiabdolmajid et al. [19, 61] also realized the mobilization of the angle of internal friction results in the mobilization of cohesive strength, equation (13) can be assumed to be more accurate for describing this scenario.

In the CWFS model, before the onset of microcracking, the frictional strength component is assumed to make no contribution to the total strength of rock, as

$$f\left(\sigma_n, \bar{\varepsilon}^{\mathrm{p}}\right)\tan\,\varphi = 0 \quad \left(\bar{\varepsilon}^{\mathrm{p}} = 0\right). \tag{14}$$

Equation (14) was obtained by assuming $\varphi = 0$ when $\bar{\varepsilon}^{\mathrm{p}} = 0$. In other words, the initial value of the angle of internal friction was assumed to be zero. However, the test results in the present study showed that the initial internal friction angle is not zero. It should be noted that two numerical studies [46, 62] adopted the CWFS model with a non-zero initial internal friction angle and obtained reasonably accurate predictions of the actual soil behavior.

6. Conclusions

By conducting triaxial compression tests in the laboratory, the parameters of cohesive strength and frictional strength of sandstone samples were measured, based on both the Mohr–Coulomb criterion and the Drucker–Prager criterion. The evolution of strength parameters of the Drucker–Prager criterion was initially calibrated in the laboratory. Five pairs of conversion formulae were reviewed, and the best formula was recommended to convert the parameters between both yield criteria. Finally, the results from this study were compared with the results from the CWFS model. The main conclusions are summarized in the following:

(1) The coefficient of pressure sensitivity α and the shearing cohesion k of the Drucker–Prager criterion can be directly obtained by conducting triaxial compression tests. This avoids the use of complicated formulae deduction.

(2) The same group of triaxial compression tests was utilized to obtain the parameters c and φ in the Mohr–Coulomb criterion and α and k in the Drucker–Prager criterion.

(3) According to the test results of sandstone, the cohesive strength parameters c and k first increased to their peak values and then decreased with increasing plastic deformation. The frictional strength parameters φ and α gradually increased at a decreasing rate after passing the initial yield point.

(4) A disadvantage of this study is that the compression tests were conducted in conventional triaxial conditions, rather than in true triaxial conditions. Thus, the influence of the variation of the intermediate stress σ_2 on the evolution of strength parameters could not be considered. In future studies, true triaxial compression tests of various rock types should be conducted to fully investigate the evolution of strength parameters.

Abbrevations

τ: Shear stress
σ: Normal stress
φ: Angle of internal friction
c: Cohesion
J_2: Second invariant of the deviatoric stress tensor
I_1: First invariant of the stress tensor
α: Coefficient of pressure sensitivity
k: Shearing cohesion
ε_{ij}: Total strain
$\varepsilon_{ij}^{\mathrm{e}}$: Elastic strain
$\varepsilon_{ij}^{\mathrm{p}}$: Plastic strain

C: Elasticity stiffness matrix
κ: Plastic internal variable
κ_i: Value of plastic internal variable at the i^{th} stage of the plastic stage
$c(\kappa)$: Mobilized cohesion with the plastic internal variable
$\varphi(\kappa)$: Mobilized angle of internal friction with the plastic internal variable
$\alpha(\kappa)$: Mobilized coefficient of pressure sensitivity
$k(\kappa)$: Mobilized shearing cohesion
σ_1: Maximum stress
σ_3: Minimum principal stress.

Data Availability

The datasets analysed during the current study are not publicly available because the authors have no rights to share it.

Conflicts of Interest

The authors declare that they have no conflicts of interest.

Acknowledgments

This work was supported by the National Natural Science Foundation of China under Grant nos. 51322404 and 51579093. Special thanks are due to the late Prof. Youquan Yin of Peking University, who greatly helped with this manuscript.

References

[1] A. Alajmi and R. Zimmerman, "Relation between the mogi and the coulomb failure criteria," *International Journal of Rock Mechanics and Mining Sciences*, vol. 42, no. 3, pp. 431–439, 2005.
[2] C. Jæger, N. Cook, and R. Zimmerman, *Fundamentals of Rock Mechanics*, Wiley-Blackwell, Oxford, Hoboken, 4th edition, 2007.
[3] J. F. Labuz and A. Zhang, "Mohr–coulomb failure criterion," *Rock Mechanics and Rock Engineering*, vol. 45, no. 6, pp. 975–979, 2012.
[4] X. L. Du, D. Lu, Q. M. Gong, and M. Zhao, "Nonlinear unified strength criterion for concrete under three-dimensional stress states," *Journal of Engineering Mechanics*, vol. 136, no. 1, pp. 51–59, 2010.
[5] B. C. Haimson and C. Chang, "A new true triaxial cell for testing mechanical properties of rock, and its use to determine rock strength and deformability of westerly granite," *International Journal of Rock Mechanics and Mining Sciences*, vol. 37, no. 1, pp. 285–296, 2000.
[6] R. Jimenez and X. Ma, "A note on the strength symmetry imposed by Mogi's true-triaxial criterion," *International Journal of Rock Mechanics and Mining Sciences*, vol. 64, pp. 17–21, 2013.
[7] X. Ma, J. Rudnicki, and B. Haimson, "The application of a Matsuoka-Nakai-Lade-Duncan failure criterion to two porous sandstones," *International Journal of Rock Mechanics and Mining Sciences*, vol. 92, pp. 9–18, 2017.
[8] K. Mogi, "Effect of the intermediate principal stress on rock failure," *Journal of Geophysical Research*, vol. 72, no. 20, pp. 5117–5131, 1967.
[9] M. Liu, Y. Gao, and H. Liu, "A nonlinear Drucker–Prager and Matsuoka–Nakai unified failure criterion for geomaterials with separated stress invariants," *International Journal of Rock Mechanics and Mining Sciences*, vol. 50, no. 2, pp. 1–10, 2012.
[10] M. Singh, A. Raj, and B. Singh, "Modified mohr–coulomb criterion for non-linear triaxial and polyaxial strength of intact rocks," *International Journal of Rock Mechanics and Mining Sciences*, vol. 48, no. 4, pp. 546–555, 2011.
[11] H. Jiang and Y. Xie, "A note on the mohr–coulomb and drucker–prager strength criteria," *Mechanics Research Communications*, vol. 38, no. 4, pp. 309–314, 2011.
[12] D. Drucker and W. Prager, "Soil mechanics and plastic analysis or limit design," *Quarterly of Applied Mathematics*, vol. 10, no. 2, pp. 157–165, 1952.
[13] Commission on Terminology Symbols and Graphic Representation of International Society for Rock Mechanics, "Terminology," 1975.
[14] L. Alejano and A. Bobet, "Drucker–prager criterion," *Rock Mechanics and Rock Engineering*, vol. 45, no. 6, pp. 995–999, 2012.
[15] A. Jaiswal and B. K. Shrivastva, "A generalized three-dimensional failure criterion for rock masses," *Journal of rock mechanics & geotechnical engineering*, vol. 4, no. 4, pp. 333–343, 2012.
[16] Y. Yin, *Stability of Rock Mechanics and Rock Engineering*, Peking University Press, Beijing, China, 2011.
[17] X. Zhang, *Plasticity of Geomaterials*, China Communications Pres, Beijing, China, 1993.
[18] V. Hajiabdolmajid, "Mobilization of strength in brittle failure of rock," PhD thesis, Queen's University, Kingston, Canada, 2001.
[19] V. Hajiabdolmajid, P. Kaiser, and C. Martin, "Mobilised strength components in brittle failure of rock," *Géotechnique*, vol. 53, no. 3, pp. 327–336, 2003.
[20] M. Jafarpour, H. Rahmati, S. Azadbakht, A. Nouri, D. Chan, and H. Vaziri, "Determination of mobilized strength properties of degrading sandstone," *Soils and Foundations*, vol. 52, no. 4, pp. 658–667, 2012.
[21] K. Lee, I. Lee, and Y. Shin, "Brittle rock property and damage index assessment for predicting brittle failure in excavations," *Rock Mechanics and Rock Engineering*, vol. 45, no. 2, pp. 251–257, 2012.
[22] H. Li, G. Xiong, and G. Zhao, "An elasto-plastic constitutive model for soft rock considering mobilization of strength," *Transactions of Nonferrous Metals Society of China*, vol. 26, no. 3, pp. 822–834, 2016.
[23] C. Martin, "The strength of massive lac du bonnet granite around underground openings," PhD thesis, University of Manitoba, Winnipeg, Canada, 1994.
[24] C. Martin, "Seventeenth canadian geotechnical colloquium: the effect of cohesion loss and stress path on brittle rock strength," *Canadian Geotechnical Journal*, vol. 34, no. 5, pp. 698–725, 1997.
[25] O. Pourhosseini and M. Shabanimashcool, "Development of an elasto-plastic constitutive model for intact rocks," *International Journal of Rock Mechanics and Mining Sciences*, vol. 66, pp. 1–12, 2014.
[26] P. Vermeer and R. Borst, "Non-associated plasticity for soils, concrete and rock," *Heron*, vol. 350, no. 3, pp. 163–196, 1984.
[27] H. Wang, W. Zhao, D. Sun, and B. Guo, "Mohr-coulomb yield criterion in rock plastic mechanics," *Chinese Journal of Geophysics*, vol. 55, no. 6, pp. 733–741, 2012.
[28] H. Zhang, S. Nunoo, D. Tannant, and S. Wang, "Numerical study of the evolution of cohesion and internal friction in rock

during the pre-peak deformation process," *Arabian Journal of Geosciences*, vol. 8, no. 6, pp. 3501–3513, 2015a.

[29] H. Zhang, D. Tannant, H. Jing, S. N. S. Niu, and S. Wang, "Evolution of cohesion and friction angle during microfracture accumulation in rock," *Natural Hazards*, vol. 77, no. 1, pp. 497–510, 2015b.

[30] K. Zhang, H. Zhou, and J. Shao, "An experimental investigation and an elastoplastic constitutive model for a porous rock," *Rock Mechanics and Rock Engineering*, vol. 46, no. 6, pp. 1499–1511, 2013.

[31] P. Zhang, X. Li, and N. Li, "Strength evolution law of cracked rock based on localized progressive damage model," *Journal of Central South University of Technology*, vol. 15, no. 4, pp. 493–497, 2008.

[32] H. Zhou, K. Zhang, and X. Feng, "Experimental study on progressive yielding of marble," *Materials Research Innovations*, vol. 15, no. s1, pp. s143–s146, 2011.

[33] Z. Chu, Z. Wu, B. Liu, and Q. Liu, "Coupled analytical solutions for deep-buried circular lined tunnels considering tunnel face advancement and soft rock rheology effects," *Tunnelling and Underground Space Technology*, vol. 94, Article ID 103111, 2019.

[34] Z. Chu, Z. Wu, Q. Liu, and B. Liu, "Analytical solutions for deep-buried lined tunnels considering longitudinal discontinuous excavation in rheological rock mass," *Journal of Engineering Mechanics*, vol. 146, no. 6, Article ID 4020047, 2020.

[35] F. Song, H. Wang, and M. Jiang, "Analytically-based simplified formulas for circular tunnels with two liners in viscoelastic rock under anisotropic initial stresses," *Construction and Building Materials*, vol. 175, pp. 746–767, 2018.

[36] K. Wu and Z. Shao, "Visco-elastic analysis on the effect of flexible layer on mechanical behavior of tunnels," *International Journal of Applied Mechanics*, vol. 11, no. 3, Article ID 1950027, 2019.

[37] K. Wu, Z. Shao, and S. Qin, "An analytical design method for ductile support structures in squeezing tunnels," *Archives of Civil and Mechanical Engineering*, vol. 20, no. 3, Article ID 91, 2020a.

[38] K. Wu, Z. Shao, S. Qin, and B. Li, "Determination of deformation mechanism and countermeasures in silty clay tunnel," *Journal of Performance of Constructed Facilities*, vol. 34, Article ID 4019095, 2020b.

[39] Z. Yao, "A method for measuring strength parameters of softening drucker-prager material," *Chinese Journal of Rock Mechanics and Engineering*, vol. 33, pp. 1187–1193, 2014.

[40] W. Chen and X. Liu, *Limit Analysis in Soil Mechanics*, Elservier, Amsterdam, Netherlands, 1990.

[41] W. Chen and A. Saleeb, *Elasticity and Plasticity*, China Architecture & Building Press, Beijing, China, 2005.

[42] X. Chu and Y. Xu, "Studies on transformation from mohr-coulomb criterion to drucker-prager criterions based on distortion energy density," *Rock and Soil Mechanics*, vol. 30, no. 10, pp. 2985–2990, 2009.

[43] R. Davis and A. Selvadurai, *Plasticity and Geomechanics*, Cambridge University Press, Cambridge, UK, 2002.

[44] Y. Zheng, Z. Shen, and X. Gong, *Generalized Plastic Mechanics-The Principles of Geotechnical Plastic Mechanics*, China Architecture and Building Press, Beijing, China, 2002.

[45] G. Xiong and J. Zhang, "Correlation analysis of relationship between druker-prager yield criteria and strength margin safety factor," *Rock and Soil Mechanics*, vol. 29, pp. 1905–1910, 2008.

[46] G. Xu and Y. Zheng, "Study on application of yield criterion in rock engineering," *Chinese Journal of Geotechnical Engineering*, vol. 12, pp. 93–99, 1990.

[47] C. Deng, G. He, and Y. Zheng, "Studies on drucker-prager yield criterions based on mohr-coulomb yield criterion and application in geotechnical engineering," *Chinese Journal of Geotechnical Engineering*, vol. 28, no. 6, pp. 735–739, 2006.

[48] X. Chen, R. Wang, and H. Deng, "The study of mohr matching D-P criteria in excavation engineering," *Opencast Mining Technology*, vol. 2010, no. 1, pp. 11–17, 2010.

[49] ASTM, "Standard test methods for compressive strength and elastic moduli of intact rock core specimens under varying states of stress and temperatures," Tech. Rep. D7012-14, American Society for Testing Materials, West Conshohocken, PA, USA, 2014.

[50] E. Fjar, R. Holt, A. Raaen, R. Risnes, and P. Horsrud, *Petroleum Related Rock Mechanics*, Elsevier, Amsterdam, Netherlands, 2nd edition, 2008.

[51] Y. Yin, *Plasticity of Geomaterials*, Peking University Press, Beijing, China, 2014.

[52] M. D. Liu and J. P. Carter, "General strength criterion for geomaterials," *International Journal of Geomechanics*, vol. 3, no. 2, pp. 253–259, 2003.

[53] X. P. Zhang, G. G. Lv, Q. S Liu et al., "Identifying accurate crack initiation and propagation thresholds in siliceous siltstone and limestone," *Rock Mechanics and Rock Engineering*, vol. 54, no. 2, pp. 973–980, 2020.

[54] M. Nicksiar and C. D. Martin, "Evaluation of methods for determining crack initiation in compression tests on low-porosity rocks," *Rock Mechanics and Rock Engineering*, vol. 45, no. 4, pp. 607–617, 2012.

[55] M. McLean and M. Addis, "Wellbore stability: the effect of strength criteria on mud weight recommendations," in *Proceedings of the all Days, Society of Petroleum Engineers of AIME*, pp. 9–17, Society of Petroleum Engineers, Houston, Texas, September 1990.

[56] C. A. M. Vee, "Use of plasticity models for predicting borehole stability," in *Proceedings of the ISRM International Symposium, Vol All Days*, Pau, France, August 1989, https://onepetro.org/ISRMIS/proceedings-pdf/IS89/All-IS89/ISRM-IS-1989-106/2015859/isrm-is-1989-106.pdf.

[57] J. Liu, M. Luan, C. Xu, J. Wang, and F. Yuan, "Study on paramteric characters of drucker-prager criterion," *Chinese Journal of Rock Mechanics and Engineering*, vol. 25, no. S2, pp. 4009–4015, 2006.

[58] L. Ma, H. Xu, Q. Tong, L. Dong, N. Zhang, and J. Li, "Post-yield plastic frictional parameters of a rock salt using the concept of mobilized strength," *Engineering Geology*, vol. 177, no. 14, pp. 25–31, 2014.

[59] J. Schmertmann and J. Osterberg, "An experimental study of the development of cohesion and friction with axial strain in saturated cohesive soils," in *Proceedings of the Research Conference on Shear Strength of Cohesive Soils*, pp. 643–694, ASCE, Boulder, CO, USA, June 1960.

[60] A. Bishop, "Shear strength parameters for undisturbed and remoulded soil specimens," in *Proceedings of the Roscoe Memorial Symposium*, pp. 3–58, Cambridge University, Cambridge, MA, USA, March 1971.

[61] V. Hajiabdolmajid, P. Kaiser, and C. Martin, "Modelling brittle failure of rock," *International Journal of Rock Mechanics and Mining Sciences*, vol. 39, no. 6, pp. 731–741, 2002.
[62] C. Wu and P. Zhang, "Analysis of numerical simulation methods for excavation failure zone of deep underground opening in hard rocks with high geostress," *Hydrogeology & Engineering Geology*, vol. 39, no. 6, pp. 35–42, 2012.